Hysteresis in One-Dimensional Reaction-Diffusion Systems

A. Rákos,[1] M. Paessens,[1] and G. M. Schütz[1,2]

[1]*Institut für Festkörperforschung, Forschungszentrum Jülich, 52425 Jülich, Germany*
[2]*Theoretische Physik I, Universität Dortmund, 44221 Dortmund, Germany*

(Received 8 May 2003; published 3 December 2003)

We introduce a simple nonequilibrium model for a driven diffusive system with nonconservative reaction kinetics in one dimension. The steady state exhibits a phase with broken ergodicity and hysteresis which has no analog in systems investigated previously. We identify the main dynamical mode, viz., the random motion of a shock in an effective potential, which provides a unified framework for understanding phase coexistence as well as ergodicity breaking. This picture also leads to the exact phase diagram of the system.

DOI: 10.1103/PhysRevLett.91.238302 PACS numbers: 82.40.–g, 02.50.Ga, 05.70.Ln, 64.60.Ht

The closely related questions of phase coexistence, ergodicity breaking, and hysteresis in noisy one-dimensional systems with short range interactions and finite local state space (such as in spin systems or vertex models) are intriguing and have received wide attention in the context of driven diffusive systems [1–8].

Recently it has been demonstrated that phase coexistence occurs in a one-dimensional driven diffusive system even in the presence of Langmuir kinetics $A \rightleftharpoons 0$ which break the bulk conservation law [9]. This mechanism is inspired by the process of motor proteins moving along actin filaments. Earlier this model was introduced as a toy model reproducing stylized facts in limit order markets [10]. The formation of a localized shock in this system which separates a domain of low particle density from a domain of high density has been studied subsequently [11,12]. However, the two different domains do not represent two possible *global* steady states. The process is ergodic even in the thermodynamic limit and no hysteresis is possible.

It is the purpose of this Letter to demonstrate the existence of hysteresis and broken ergodicity (in the thermodynamic limit) in a driven diffusive system without bulk conservation law. Surprisingly, adding noise which is on average spatially homogeneous (a nonconservative reaction process) to a conservative spatially homogeneous nonequilibrium system with a nonvanishing particle current leads to a *space-dependent* effective potential which determines the stationary position of the shock connecting low-density and high-density regions. In the absence of this noise, i.e., in the usual totally asymmetric exclusion process (TASEP), the shock performs an unbiased random walk in the coexistence region and hence is unlocalized, whereas suitably chosen reaction kinetics may create a variety of effective potentials which lead to broken ergodicity by localizing the shock.

To be specific we investigate the TASEP augmented by nonconservative reaction kinetics. The TASEP is a stochastic model of diffusing particles on a one-dimensional lattice with a hopping bias in one direction [8]. Each site from 1 to L is either empty ("$\varnothing$") or occupied by one particle ("A"). In the bulk particles hop stochastically from site i to $i+1$ with unit rate, provided that the target site is empty. The boundaries act as particle reservoirs with densities ρ_- on the left and ρ_+ on the right: On site 1 particles are created with rate ρ_-, provided the site is empty, which corresponds to a particle hopping from the left reservoir onto the first site. Particles on site L are annihilated with rate $1-\rho_+$, corresponding to a particle hopping from the last site into the right reservoir.

In our model particles also undergo the following reaction process: On a vacant site enclosed by two particles a particle may be attached with rate ω_a, and a particle enclosed by two other particles may be detached with rate ω_d. This process can be symbolically written as $A\varnothing A \rightleftharpoons AAA$ and may be interpreted as activated Langmuir kinetics. Without the TASEP dynamics the stationary density of this process is either $K = \omega_a/(\omega_a + \omega_d)$ or zero, with no correlations [13]. As in previous work, we consider the physically interesting case when $L \to \infty$, and these rates are proportional to $1/L$ [9–12]. Hence we define renormalized rates

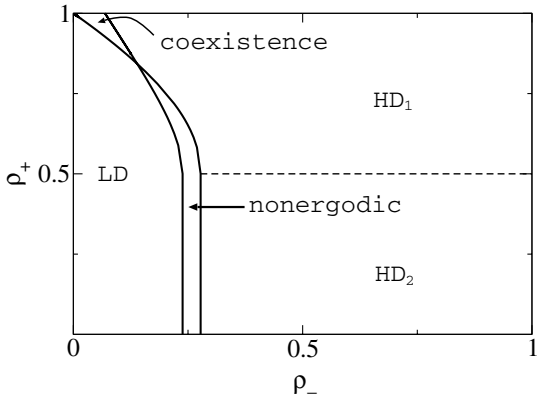

FIG. 1. Phase diagram for $\Omega_a = 0.7$ and $\Omega_d = 0.1$ with two high-density phases (HD1, HD2), a low-density phase (LD), a coexistence phase, and the nonergodic phase.

 © 2003 The American Physical Society

$$\omega_a = \Omega_a/L, \qquad \omega_d = \Omega_d/L, \tag{1}$$

where Ω_a and Ω_d are kept constant while $L \to \infty$. For other choices of the attachment-detachment (AD) rates the dynamics is governed by either the TASEP [$\omega_{a,d} < \mathcal{O}(1/L)$] or the AD process [$\omega_{a,d} > \mathcal{O}(1/L)$].

We find a stationary phase diagram of the model with five distinct phases (Fig. 1). The stationary density profile ρ_i is not constant as a function of lattice site i. Yet some of the phases are comparable to those of the usual TASEP with open boundaries [14,15]: in the high-density phases (HD1 and HD2) one finds $\rho_i > 1/2$, while in the low-density phase (LD) $\rho_i < 1/2$. In HD1 the bulk density profile is dependent on ρ_+, while it is independent of both boundaries in HD2 as in the maximal current phase of the TASEP. On the other hand, two additional phases exist: A coexistence phase which is characterized by a stable shock position, i.e., a jump in the density profile which is localized at a certain position in the bulk of the system. The shock connects a low-density domain to its left with a high-density domain to its right, as known from related models studied previously [9,11]. Notice that in the usual TASEP there is a coexistence line in the phase diagram with a *nonlocalized* shock. In a different parameter regime we find a novel phase with an unstable shock position in the bulk. In this phase both the LD and HD states are stable (if $L \to \infty$) which implies that ergodicity is broken in the thermodynamic limit. Although for finite systems a transition between the two states is possible, the mean lifetime of each steady state is exponentially large in the system size L (see below). We note that this is not a spontaneous symmetry breaking since there is no symmetry relating the two metastable states. This phase has no analog in the TASEP with open boundaries.

Hysteresis in this nonequilibrium setting was observed by measuring the space-averaged density $\bar{\rho}$ along the curve of constant $\rho_+ = 0.45$ while changing ρ_- in such a way that the system starting from the LD phase passed through the nonergodic phase and ended up in the HD2 phase. Then the process of changing ρ_- was reversed. A relevant parameter in hysteresis phenomena is the speed of sweeping: in our simulations ρ_- was changed by 10^{-4} in every k Monte Carlo (MC) steps ($k = 500, 1500, 5000$). A time average was not taken, and $\bar{\rho}$ was measured in every k step. In Fig. 2 one can see the resulting hysteresis loops. We found that the hysteresis loop inflates with increasing speed which is reminiscent of hysteresis in usual magnetic systems.

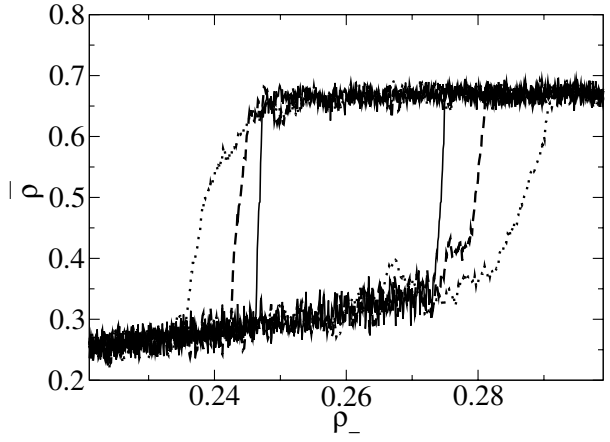

FIG. 2. Hysteresis plot for $L = 2000$, $\Omega_a = 0.7$, $\Omega_d = 0.1$, $\rho_+ = 0.45$. ρ_- was changed by 10^{-4} in every 5000 (solid line), 1500 (dashed line), and 500 (dotted line) MC steps. The hysteresis loop gets wider as the speed of changing ρ_- is increased.

To rationalize these observations we first consider the hydrodynamic limit on the Euler scale; i.e., we take $L \to \infty$ while the lattice constant is scaled by $a = 1/L$ and the time by $t = t_{\text{lattice}}/L$. Thus the spatial coordinate $x = i/L$ becomes continuous. Following the line of arguments of Ref. [11] the hydrodynamic equation for the density takes the form

$$\frac{\partial}{\partial t}\rho(x,t) + \frac{\partial}{\partial x} j(\rho) = S(\rho), \tag{2}$$

with the exact current $j(\rho) = \rho(1-\rho)$ of the TASEP and the cubic source term

$$S(\rho) = \Omega_a \rho^2 (1-\rho) - \Omega_d \rho^3, \tag{3}$$

resulting from the activated Langmuir kinetics. For the stationary state $\partial_t \rho(x,t) = 0$ holds, and using $\partial_x j = \partial j/\partial\rho \cdot \partial\rho/\partial x$ we obtain

$$v_c(\rho)\frac{\partial \rho(x)}{\partial x} = S(\rho), \tag{4}$$

with the collective velocity $v_c = \partial j/\partial\rho$. This nonlinear differential equation can be integrated analytically and yields the flow field

$$x(\rho) = -\frac{1}{\Omega_a \rho} + \frac{\Omega_a - \Omega_d}{\Omega_a^2} \ln\left|\frac{1}{K} - \frac{1}{\rho}\right| + c \tag{5}$$

with an integration constant c.

As the differential equation is of first order and the boundary condition fixes the density at two positions, following a line of the flow field does not represent a solution of the boundary problem in general. In the original lattice model this inconsistency is resolved by the appearance of shock and/or boundary layers as described in [11]. Apart from the discontinuities the stationary density profile follows the flow field of Eq. (4).

In order to understand quantitatively the selection of the stationary shock position (which determines the phase diagram) and also to explain the phenomenon of hysteresis from a microscopic viewpoint, we describe the dominant dynamical mode of the particle system in terms of the random motion of the shock. To this end we generalize the approach of [16] and introduce space-dependent hopping rates

$$w_{x\to x+a} = \frac{j_R(x)}{\rho_R(x) - \rho_L(x)}, \qquad w_{x+a\to x} = \frac{j_L(x)}{\rho_R(x) - \rho_L(x)}, \tag{6}$$

for jumps of the shock over a lattice constant a. Here the indices L and R denote the solutions [lines of the flow field (5)] on the left and right, respectively, of the shock. Similar hopping rates are used in [12]. The space-dependent hopping rates furnish us with the picture of a random walker in an effective energy landscape $E(x)$ inside a finite box. The energy landscape is generated by the interplay of the particle current with the reaction kinetics. In this way we relate the original nonequilibrium many-particle system to an equilibrium single-particle model. Let $p(x)$ be the equilibrium probability of the shock being at position x. Then due to detailed balance

$$\frac{w_{x\to x+a}}{w_{x+a\to x}} = \frac{p(x+a)}{p(x)} = \exp[-E(x+a) + E(x)], \tag{7}$$

which defines the energy landscape.

The potential $E(x)$ is a monotonically increasing (decreasing) function for the HD (LD) phase (Fig. 3). This implies that although there are fluctuations the shock is always driven to the left (right) boundary. In the coexistence phase there is a global minimum in the bulk resulting in a stable shock position (Fig. 3) at a macroscopic distance from the boundaries. Here the dynamics can be well approximated by a random walker in a harmonic potential which gives a Gaussian distribution for the shock position. Hence the width of the shock distribution is proportional to $\sqrt{L}$ [13] which was also found in [9,12] for the TASEP with Langmuir kinetics.

The nonergodic phase is characterized by a global energy *maximum* in the bulk (Fig. 3), leading to an unstable bulk fixed point of the shock. The two minima at the left and right boundaries correspond to the two stable stationary states. Starting with an initial condition close to 1 of the minima, the random walker will drift most likely into this local minimum and stay in its vicinity for a time of the order of the mean first passage time $\bar{\tau}$ before it traverses to the other minimum. This leads to hysteresis. Using a formula for the mean first passage time derived by Murthy and Kehr [17], one expects that $\bar{\tau}$ grows exponentially with the system size L. Moreover, one expects the transition from one minimum to the other to be a random Poisson process with an average waiting time $\bar{\tau}$.

This simple one-particle picture is well borne out by MC simulations. For judiciously chosen parameters it is possible to perform simulations to times much larger than $\bar{\tau}$. Using multispin coding [18] for the MC algorithm, rather good statistics become available for the waiting time τ (the time the system spends in one of the stationary states before switching to the other). For tracing the position of the shock we use the second-class particle technique [19], which allows for tracking the flow of local fluctuations required to determine the shock position on the lattice scale [13].

We measured the position of the second-class particle as a function of time: a typical realization is shown in Fig. 4.

As shown in Fig. 5 the numerically determined cumulative distribution function $\Phi(t) = P(\tau < t)$ of the waiting time τ is hardly distinguishable from the expected exponential distribution

$$\Phi(t) = 1 - \exp(-t/\bar{\tau}). \tag{8}$$

With this picture of a moving shock in mind and using the expression (5), it is also possible to derive the exact

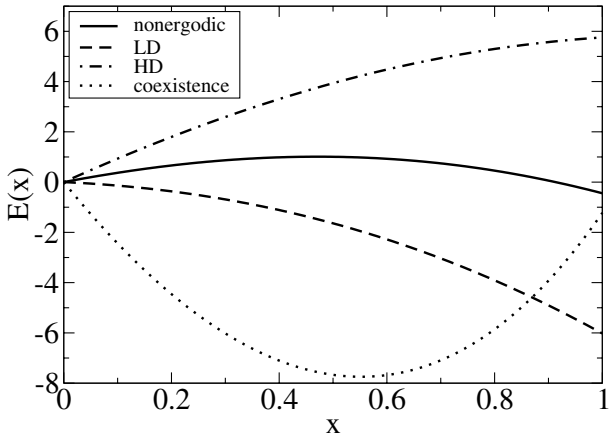

FIG. 3. Examples for the energy landscape in four phases. Note that in the HD and LD phases $E(x)$ can be either convex or concave.

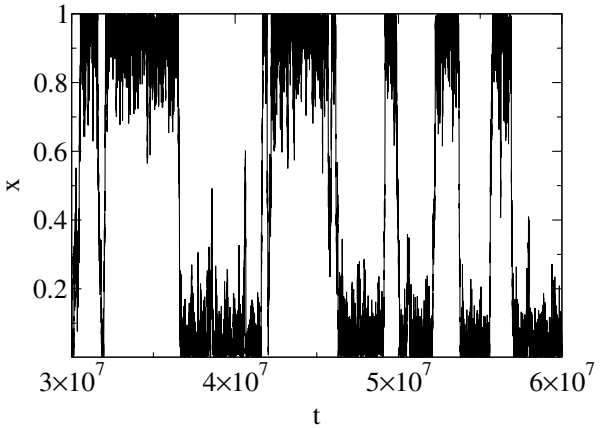

FIG. 4. Snapshot of the time evolution of the scaled position of the second-class particle for $L = 1000$, $\rho_- = 0.2705$, $\rho_+ = 0.63$, $\Omega_a = 0.5$, $\Omega_d = 0.1$. A position of the second-class particle near the left boundary ($x \approx 0$) corresponds to the high-density state, while a position near the right boundary ($x \approx 1$) corresponds to the low-density state.

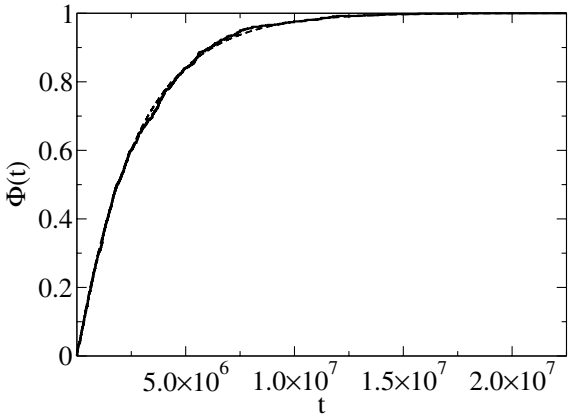

FIG. 5. Numerically determined cumulative distribution of the transition times from the upper state to the lower (solid line) compared to the exponential distribution (dashed line) with parameters as in Fig. 4. Similar results are found for the transition in the other direction, but with a different $\bar{\tau}$ [13].

phase transition lines defining the phase diagram presented above by adapting the arguments of [11]. The sign of the slope of the energy profile, i.e., the stability of the shock position, can be analyzed by considering the average shock velocity

$$v_s(x) = \frac{j_R(x) - j_L(x)}{\rho_R(x) - \rho_L(x)}. \tag{9}$$

A shock position at the boundary is stable when it is driven towards the boundary; i.e., $v_s(0) < 0$ at the left boundary, and $v_s(1) > 0$ at the right boundary. Thus the lines separating the phases are calculated by comparing the values of $\rho_L(x)$ and $\rho_R(x)$ at the positions $x = 0, 1$. In the high- and low-density phases, respectively, the energy profile has a unique minimum at one of the boundaries. In the nonergodic phase the energy profile exhibits two minima at the boundaries, so that the shock position is stable at both of them.

We mention in passing that the analytical treatment predicts a phase near the intersection point of the two nontrivial lines in the phase diagram with an energy profile having a minimum and also a maximum in the bulk. However, the region in the (ρ_-, ρ_+) space is rather narrow and the energy landscape is too flat to observe this in simulations.

To conclude, we have presented a simple nonequilibrium system with local nonconservative dynamics and finite local state space which exhibits ergodicity breaking and hysteresis in the thermodynamic limit, in the usual sense that in finite volume the sojourn time in two metastable steady states increases exponentially with system size. We stress that the two different stationary distributions are not ordered states in which the activated Langmuir reaction kinetics would be dynamically suppressed. The description of the nonequilibrium many-body dynamics in terms of a collective single-particle mode moving under equilibrium conditions yields the exact stationary phase diagram as well as the numerically verified flipping process between the metastable states of the finite system. Details of the flipping dynamics will be presented elsewhere [13].

A. Rákos thanks the Deutsche Forschungsgemeinschaft (DFG) for financial support.

[1] M. R. Evans, D. P. Foster, C. Godrèche, and D. Mukamel, J. Stat. Phys. **80**, 69 (1995).
[2] M. R. Evans, Y. Kafri, H. M. Koduvely, and D. Mukamel, Phys. Rev. Lett. **80**, 425 (1998).
[3] R. Barlovic, L. Santen, A. Schadschneider, and M. Schreckenberg, Eur. Phys. J. B **5**, 793 (1998).
[4] P. F. Arndt, T. Heinzel, and V. Rittenberg, J. Phys. A **31**, L45 (1998).
[5] Y. Kafri, E. Levine, D. Mukamel, G. M. Schütz, and J. Török, Phys. Rev. Lett. **89**, 035702 (2002).
[6] O. M. Braun, B. Hu, A. Filippov, and A. Zeltser, Phys. Rev. E **58**, 1311 (1998).
[7] D. Helbing, D. Mukamel, and G. M. Schütz, Phys. Rev. Lett. **82**, 10 (1999).
[8] G. M. Schütz, in *Phase Transitions and Critical Phenomena*, edited by C. Domb and J. Lebowitz (Academic, London, 2001), Vol. 19.
[9] A. Parmeggiani, T. Franosch, and E. Frey, Phys. Rev. Lett. **90**, 086601 (2003).
[10] R. D. Willmann, G. M. Schütz, and D. Challet, Physica (Amsterdam) **316A**, 430 (2002).
[11] V. Popkov, A. Rákos, R. D. Willmann, A. B. Kolomeisky, and G. M. Schütz, Phys. Rev. E **67**, 066117 (2003).
[12] M. R. Evans, R. Juhasz, and L. Santen, Phys. Rev. E **68**, 026117 (2003).
[13] A. Rákos and M. Paessens (to be published).
[14] G. Schütz and E. Domany, J. Stat. Phys. **72**, 277 (1993).
[15] B. Derrida, M. R. Evans, V. Hakim, and V. Pasquier, J. Phys. A **26**, 1493 (1993).
[16] A. B. Kolomeisky, G. M. Schütz, E. B. Kolomeisky, and J. P. Straley, J. Phys. A **31**, 6911 (1998).
[17] K. P. N. Murthy and K.W. Kehr, Phys. Rev. A **40**, 2082 (1989); **41**, 1160 (1990).
[18] G. T. Barkema and M. E. J. Newman, *Monte Carlo Methods in Statistical Physics* (Clarendon Press, Oxford, 1999).
[19] P. A. Ferrari, C. Kipnis, and E. Saada, Ann. Probab. **19**, 226 (1991).